Investigation of Particle Motion in a Swirling Fluidized Bed using Particle Imaging Velocimetry

by

Chin Swee Miin

Dissertation submitted in partial fulfilment of
the requirement for the
Bachelor of Engineering (Hons)
(Mechanical Engineering)

May 2012

Universiti Teknologi PETRONAS
Bandar Seri Iskandar
31750 Tronoh
Perak Darul Ridzuan

CERTIFICATION OF APPROVAL

Investigation of Particle Motion in a Swirling Fluidized Bed using Particle Imaging Velocimetry

by

Chin Swee Miin

A project dissertation submitted to the
Mechanical Engineering Programme
Universiti Teknologi PETRONAS
in partial fulfillment of the requirement for the
BACHELOR OF ENGINEERING (Hons)
(MECHANICAL ENGINEERING)

Approved by,

_____
(AP. Ir. Dr. Shaharin Anwar Sulaiman)

UNIVERSITI TEKNOLOGI PETRONAS

TRONOH, PERAK

May 2012

CERTIFICATION OF ORIGINALITY

This is to certify that I am responsible for the work submitted in this project, that the original work is my own except as specified in the references and acknowledgements, and that the original work contained herein have not been undertaken or done by unspecified sources or persons.

_____
CHIN SWEE MIIN

ABSTRACT

Fluidized bed is an advanced technology which possesses a number of characteristics ideal for a wide variety of industrial applications due to its advantages over many existing technologies in industry. However, conventional fluidized bed used in most of the industry today has certain drawbacks which affect the efficiency of the bed. Swirling Fluidized Bed (SFB) is one of the evolutions of fluidized bed, which has the potential for solving many drawbacks of conventional fluidized bed. Nonetheless, limited research has been done on this bed as compared to other versions of fluidized bed, thus a lot of problems occurred when come to scaling up to commercial size. This was mainly due to the lack of understanding of the particle dynamic characteristics of the bed. Most of the research studied the overall bed characteristics especially the pressure drop. There is limited study on the velocity and particle motion. Furthermore, available literature concentrates only analytical model and simulation results. No published experimental information is available for the analysis of the particle velocity. Thus, the objectives of the present study are to investigate particle motion in a swirling fluidized bed and to study the effect of air flow rate, bed weight, blade angle, particle size and particle shape on the fluidized particle velocity. The particle motion of the SFB is studied by using Particle Imaging Velocimetry (PIV) in an experimental model of SFB. The experiments were carried out with bed weight varied from 500 g to 1500 g with only stable swirling regime was studied and the velocity of the top layer particles was evaluated. From the study, it is found that the particle velocity increases with air flow rate at shallow bed and as bed weight is increased, particle velocity decreases by higher occurrence of vigorous bubbles. It is also observed that particle velocity decreases less than 18% with 3^{o} increment in the blade angle. Small particle yields lower minimum swirling air superficial velocity which means preferable for saving energy, but with constraint of shallow bed. Particle with elongated shape possesses short range of stable swirling due to easier occurrence of bubbling. The results of this project give a better understanding of the particle velocity and motion which can provide a great contribution towards designing the fluidized bed especially for catalyst activity, coating and drying.

ACKNOWLEDGEMENT

First and foremost, the author would like to express her highest gratitude to her supervisor, AP. Ir. Dr. Shaharin Anwar Sulaiman, for all the motivation, knowledge and valuable advices that he has given. The guidance and supervision from him have granted her many opportunities to explore, learn and experience throughout the project.

The author is also very grateful to Professor Dr. Vijay R. Raghavan, Professor Dr. Morgan R. Heikal, Dr. Yohannes T. Anbese and Vinod Kumar V. who had provided the author constructive advices and valuable assistances in accomplishing the project.

This project will not be successful without the technical helps from the laboratory assistants. They are Mr. Jani, Mr. Khairul, Mr. Hasri and Mr. Mior. Their kindness and hospitality provide the author a comfortable and conducive working environment.

Finally, the author would like to extend her appreciation to Universiti Teknologi PETRONAS for providing the facilities and many learning opportunities, and to her family and friends who constantly support her throughout the project.

TABLE OF CONTENT

LIST OF FIGURES

LIST OF TABLES

CHAPTER 1

INTRODUCTION

1.1 Background of Study

Fluidized bed is an advanced technology which possesses a number of characteristics ideal for a wide variety of industrial applications such as combustion, gasification of biomass fuels, drying, oxidation, metal surface treatment, catalytic and thermal cracking, coating etc (Howard, 1989). It is a technology which uses the technique of suspending solids through gas and gives the solids fluid-like behaviour. This technology has gained its position in many chemical and mechanical processes due to its high efficiency and flexibility.

Its advantages include good particle mixing, uniform thermal distribution, good adaptability to high-pressure and temperature operations, continuous particle addition or removal and easy transport of particles (Yang, 2003). Furthermore, the lack of moving parts in fluidized bed compared to other conventional technology enables the reduction of maintenance costs and down time. These advantages significantly improve many applications of the fluidized bed. One of the best instances is fluidized bed combustor. The high efficiency of combustion in fluidized bed allows the burning of fuels in low temperature and low excess air which results in flue gases with low amounts of carbon dioxide and pollutants. It is an environmentally favourable technology and solution to many industrial applications nowadays.

The first fluidization research appeared in 1940s when people just treated the bed as a black box by merely measuring the effective diffusivity, effective thermal conductivity and reaction rates (Horio, 2011). To date, after 70 years of research, hundreds of fluidized bed concepts and configurations, mostly for particular purposes, have been specifically designed and produced for actual industrial applications. The types of fluidized bed include the basic conventional, centrifugal, circulating, vortexing, rotating distributor, rotating with static geometry, toroidal (Torbed), swirling and conical swirling.

1.2 Problem Statement

Today, conventional fluidized bed used in most of the industry utilizes perforated distributor in which the air flows directly upward to suspend the particles as shown in Figure 1.1. This fluidized bed has several drawbacks such as the momentum of particles in axial (upward) direction only, elutriation, limited particle size and high pressure drop.

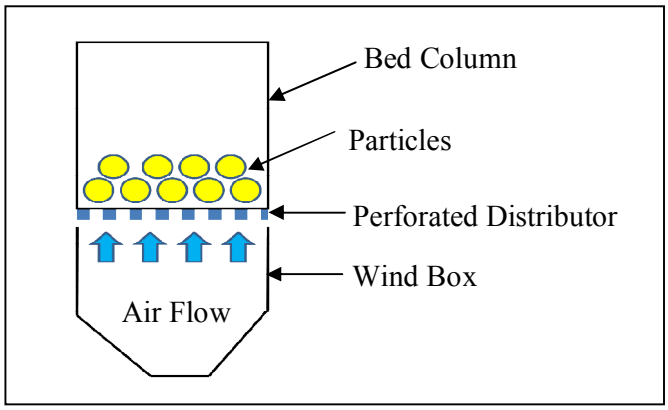

Figure 1.1 Conventional fluidized bed

Therefore, swirling fluidized bed (SFB), shown in Figure 1.2, is a new variant in the technique of fluidized bed operation evolved from efforts to overcome the disadvantages of the conventional fluidized bed. It is worth studied due to its high potential to overcome many of the deficiencies in conventional fluidized bed. SFB minimizes momentum in axial direction and transfers it into radial and tangential directions. It provides excellent particles mixing, reduces elutriation, allows wider range of particle size and lowers pressure drop.

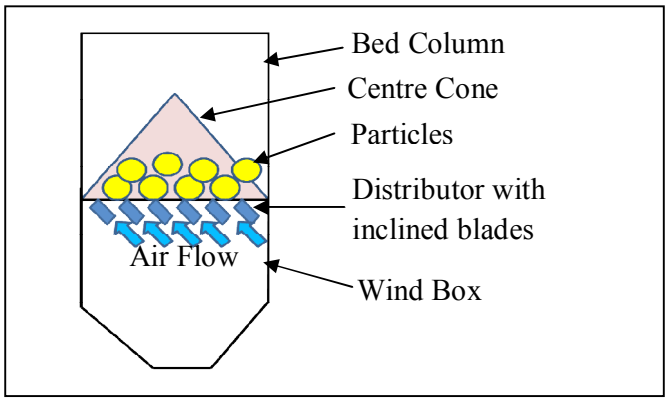

Figure 1.2 Swirling fluidized bed

Even though SFB has been implicated, it has not been fully developed and a lot of problems such as unexpected material wastes, unstable heat transfer rate, corrosion/erosion etc. have occurred when the fluidized bed is scaled up to the commercial size (Lee and Liu, 2004). This is mainly due to the lack of understanding of the particle dynamic characteristics of the bed. Published information on the behaviour of the bed is scanty. Most of the researches study the overall bed characteristics especially the pressure drop. There is limited study on the velocity and particle motion in the bed. Furthermore, available literatures are only analytical model and simulation results. No published experimental information is available for the analysis of the particles velocity and for the validation of the analytical model of SFB.

Thus, in order to fill up this gap, experiments are required to study the particle behaviour, which is important in determining the efficiency of the SFB especially in particle mixing, heat and mass transfer of the bed. A better understanding of the particle velocity and motion can be a great contribution towards designing the fluidized bed especially for catalyst activity, coating, drying and many other processes, which require the knowledge of the fluidized particle velocity.

1.3 Objectives

The objectives of the present study are:

(i) To investigate particle motion in a swirling fluidized bed in relation to air superficial velocity by mapping the trajectory of the bed particles.

(ii) To study the effect of bed weight, blade angle, particle shape and particle size on the fluidized particle velocity.

1.4 Scope of Study

To study the trajectory and velocity of the fluidized bed particles, an experiment using an accurate and effective visualization technique and velocity measuring technique, Particle Imaging Velocimetry (PIV), is conducted. This

requires the utilization of a high speed camera and PIV software which involve natural light imaging, post-processing and analysis. Besides, an overall study of the swirling fluidized bed is accomplished in order to understand the relation between the velocity/trajectory and other parameters related to the fluidized bed.

1.5 Significance of Project

Hydrodynamic studies of SFB are essential to provide information on the basic flow patterns, mixing, particle attrition behaviour and mass and heat transfer for the design of the fluidized bed. The analysis of this study serves as a reference for the validation of the analytical model of the bed. By knowing the effects of the parameters which have been studied, the motion of the particles can be predicted and improvements can be done on the applications of the bed. This contributes to the design of the scaled-up model SFB for industrial applications. Besides, from the data of the particle velocity, slip velocity on the particle which has always been unknown can be determined. This helps to increase understanding of the hydrodynamics characteristics of SFB and to predict heat and mass transfer rates between gas and particles.

CHAPTER 2

LITERATURE REVIEW AND THEORIES

2.1 Fluidization

Fluidization is a process which transforms a bed of solid particles into fluid-like properties through suspension in a gas or liquid. The fluidized state happens when the gravitational force on the solid particles is overcome by the fluid drag due to the injected gas or liquid as shown in Figure 2.1. The contact between the solid particles and fluid gives characteristics of fluid to the solids which enables the solids to flow freely under gravity and to be pumped using fluid-typed technologies. In other words, the solids are easy to transport and handle.

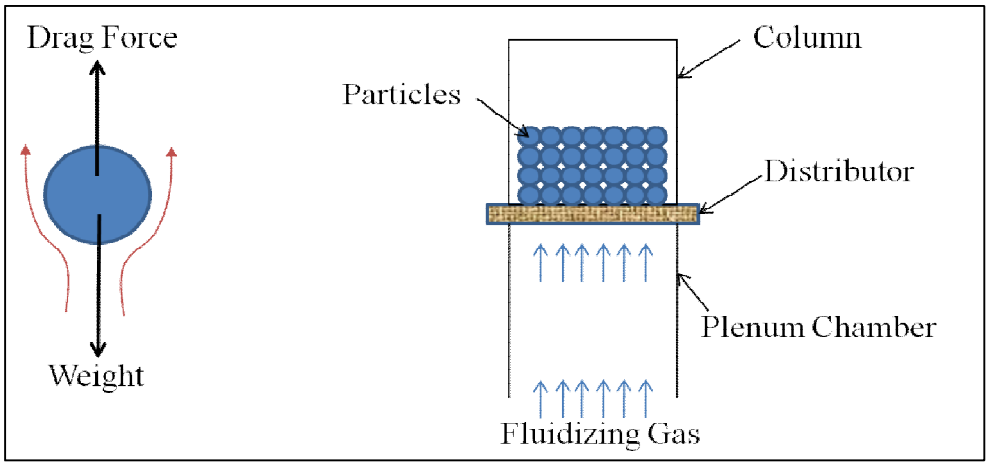

Figure 2.1 Force balance between gravitational force and drag force on a particle

In the study of fluidization, it is very impractical to test a wide variety of powder as one of the variables of the research. Furthermore, there is a huge tendency to cause confusion when the conclusion from a research is applied to another fluidized bed which uses completely different properties of particles. Thus, to overcome this problem, Geldart (1973) proposed a method of classification which is now named as "Geldart Grouping". This classification falls into four clearly recognizable groups (A, B, C and D), characterized by density difference and mean particle size of the powders as shown in Figure 2.2. Each group exhibits different

behaviour during fluidization. According to Geldart (1973), powders in group A exhibit dense phase expansion after minimum fluidization whereas powders in group B bubble at the minimum fluidization velocity; powders in group C are difficult to fluidize and those in group D are of large size and density requires most energy to fluidize and spout readily.

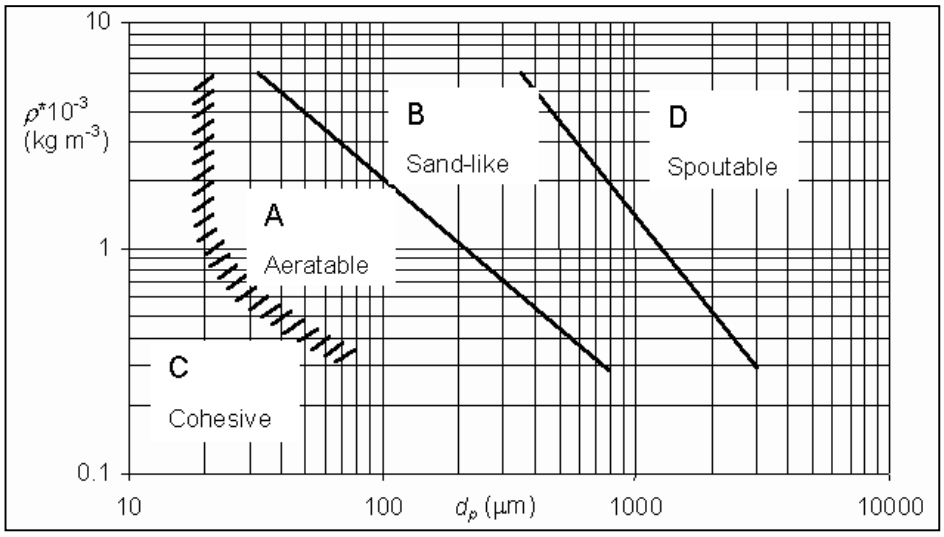

Figure 2.2 Geldart's classification of powder according to fluidization properties (Geldart, 1973)

2.2 Swirling Fluidized Bed

Many attempts have been made to develop a fluidized bed which can be used to fluidize as many types of powder as possible efficiently and to improve the performance of the conventional fluidized bed. This has resulted in the development of a lot of different fluidized beds such as centrifugal, circulating, vortexing, rotating distributor, rotating with static geometry, toroidal (Torbed), swirling, conical swirling etc (Kumar and Raghavan, 2011). Swirling fluidized bed is a relatively new variant of fluidized bed and it has high potential in solving most of the shortcomings in conventional fluidized bed.

Swirling fluidized bed (SFB), as indicates by its name, is a type of fluidized technique which introduces swirling motion to the particles of a bed. Typically, there

are several methods of achieving swirling fluidization: secondary injection of fluidizing medium into the freeboard tangentially (Sowards, 1978), utilization of a distributor which provides inclined injection into the bottom of the bed (Paulose, 2006) and rotation of the distributor or rotation of the bed column (Sobrino et al., 2008). Figure 2.3 shows the model of a swirling fluidization using an annular blade distributor (Sreenivasan and Raghavan, 2002).

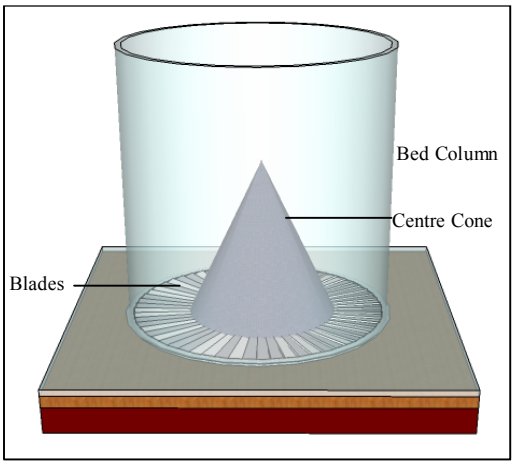

Figure 2.3 Configuration of swirling fluidized bed using an annular blade distributor

2.2.1 Working Principles

In SFB with annular blade distributor, an inclined injection of gas will be introduced through the distributor blades into the bottom of the bed. The jet of gas entering the bed can be resolved into two components of velocity, which are the vertical component ($V \sin\vartheta$) and horizontal component ($V \cos\vartheta$). The vertical component causes fluidization while the horizontal component is responsible for the swirl motion of the bed particles.

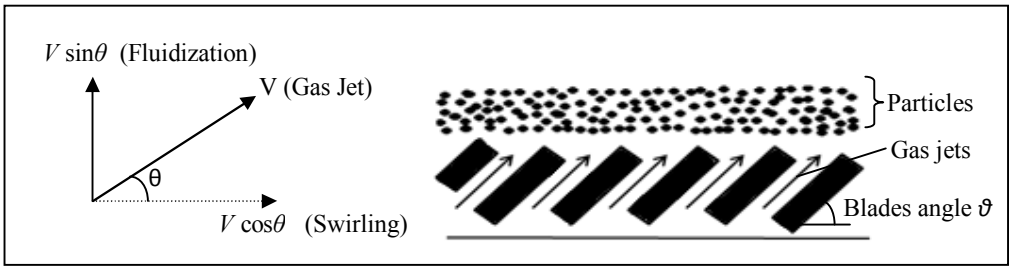

Figure 2.4 Principle of particle movement in swirling fluidized bed

According to Sreenivasan and Raghavan (2002), there are basically four regimes of operation that can be found in SFB with increasing gas velocity as shown in Figure 2.5. The first regime is known as fixed bed in which the particles are not fluidized because the gas drag force is not sufficient to overcome the weight of the particles. As gas velocity increases, minimum fluidization will be achieved with gas bubbles form above distributor and this regime is called bubbling regime (second regime). The third regime involves the formation of dune and wave motion with the increment of gas velocity. In this regime, there are two zones which are swirling zone and static zone. The swirling zone carries the particles with it and deposits them at the boundary of the static zone while at the other boundary of the static zone, particles gets depleted which reduces the bed height. This causes wave motion of the particles. On further increasing the gas velocity, dune formation is weakened and finally disappears. However, the swirling region gets wider and results in steady state swirling motion of the particles. This forth regime is only applicable to shallow bed. If the bed is deep enough, two layers of regime will be formed where a thin continuously swirling layer is observed at the bottom of the bed and a vigorously bubbling layer will be on the top.

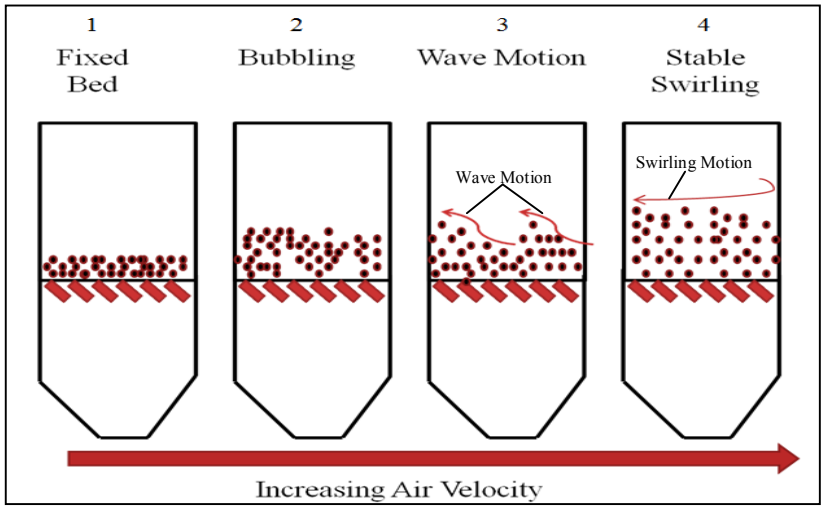

Figure 2.5 Different regimes of operation of swirling fluidized bed

2.2.2 Advantages

Unlike conventional fluidized bed, SFB minimizes the axial momentum transferred to the particle with a larger fraction of momentum being transferred radially and tangentially. This increases the mixing of the particles and eventually increases the transport properties of the particles. The swirling motion enables gas velocity to be increased to high values with little elutriation. Furthermore, large particles in Geldart 'D' type, which are usually difficult to fluidize in a conventional fluidized bed can be effectively fluidized in SFB.

This new variant of fluidized bed has not received much attention in research. Systematic studies of SFB are relatively limited even though its principles have already been used in commercial equipment. Several studies have confirmed the advantages of SFB as compared to conventional fluidized bed. Ouyang and Levenspiel (1986) proposed a basic swirling fluidized bed model with a spiral distributor, made of overlapping vanes which are shaped as sectors of a circle. They evaluated the characteristics of this distributor such as pressure drop, quality of fluidization and heat transfer coefficient between the bed and an immersed surface which showed improvement compared to conventional fluidized bed. Chyang and Lin (2002) further studied the influence of the swirling fluidizing pattern of another better and new design, which had a multi-horizontal nozzle distributor. It showed a remarkable improvement too, with better fluidization quality and reduction of elutriation.

Another research was done by Shu et al. (2000) who studied the hydrodynamics of a toroidal fluidized bed (Torbed) reactor which was similar to SFB. It was reported that the Torbed reactor showed great flexibility in thermal processing and the hydrodynamic behaviour was essentially predictable at ambient temperature. Kaewklum et al. (2009) again reported the hydrodynamics behaviour of the SFB with annular-blade distributor. High combustion efficiency and low emissions were concluded.

2.2.3 Bed Pressure Drop

Pressure drop of the fluidized bed is an important factor which has been studied by many researchers because it determines the energy consumption of the bed. Similar to Torbed which was studied by Shu et al. (2000), another version of swirling fluidized bed with annular bed with inclined injection of gas through distributor blades was studied by Sreenivasan and Raghavan (2002) who found that the bed pressure drops in the swirling mode with increasing air velocity. Further research is continued with the concern of the pressure drop of the bed. Paulose (2006) studied more details into the hydrodynamics of SFB particularly on the percentage area of opening, angle of air injection and the percentage of the useful area of the distributor. The distributor pressure drop was found to be decreasing with increase in the percentage area of opening. Besides, Batch and Raghavan (2011) also found that larger particles had lower pressure drop and high bed load increased pressure drop. Higher blade overlapping angle and number of blades (lower FOA) gave lower pressure drop which matched with the findings of Paulose (2006).

2.2.4 Particle Velocity

Particle velocity of the swirling bed is also another important hydrodynamic characteristic which must not be neglected as it is one of the factors which determine the design and performance of the bed. Lee and Liu (2004) did a study on the bed expansion and analysis on the particle velocity in a swirling fluidized bed combustor cold model which used the injection of secondary air for the creation of the swirl motion. It was found that the secondary air injection did not affect the bed expansion but increased the particle velocity. However, the particle velocity analysis was done based on the images taken from the wall side which does not really give much information regarding the angular velocity and swirl motion of the swirling particles.

An analytical model for the prediction of the hydrodynamics behaviour of the bed including the pressure drop and angular velocity of particles was developed by Vikram et al. (2003) and Raghavan et al. (2004). Vikram et al. (2003) assumed that the angular velocity of the particles remains constant across the bed height which means the model cannot predict the variation of the angular velocity and pressure

drop according to the bed height and radial distance. This model was further developed by Raghavan et al. (2004) who eliminated the lumped model used by Vikram but introduced two-dimensional model (axial and radial directions) which gave a more realistic prediction of the hydrodynamic behaviour of SFB. These are the only two analytical models that have been published regarding this SFB with annular distributor.

Till now, there has been no published experimental study on the particle motion or behaviour especially particle velocity of SFB with annular blade distributor. The lack of this information affects and delays the design and manufacturing of the swirling fluidized bed when it is to be scaled up to the commercial unit. For instance, in the application of coating, the velocity of the particle and the liquid spraying rate are very important for the design of optimized condition for the fluidized bed. However, without proper setting, the liquid spraying rate may exceed the rate of particle motion, and thus may cause the coated particles to collide before the liquid completely dries and thus agglomeration of particles will occur. Furthermore, the analytical models suggested by researchers such as Vikram et al. (2003) and Raghavan (2004) may contribute to the development of commercial SFB but without validation from data of the actual particle velocity from experiments, the proposed model cannot be confirmed and be utilized.

Therefore, an experimental study of the particle motion and velocity in SFB will assist in the realization of commercial SFB unit by providing more information and understanding of the particle hydrodynamic characteristics. Besides, the agreement between the experimental result and analytical model will help in contributing empirical equations for the design and control of scaled up commercial SFB.

CHAPTER 3

METHODOLOGY

This chapter is divided into several sections to discuss in details of the methodology used in this project. Section 3.1 elaborates the method selected to study the particle motion in the swirling fluidized bed. Section 3.2 explains the planning of the experiment with several parameters or factors chosen to study their effects on the particle velocity while Section 3.3 gives illustration of the experiment set-up and the equipments or tools required. Section 3.4 consists of the explanation on the procedures, which were taken in Particle Imaging Velocimetry and Section 3.5 is the further explanation on the method to analyze and interpret the data obtained from the particle imaging velocimetry. To ensure that the project could be done within the time period given, Gantt Charts shown in Figure 3.1 and Figure 3.2 were followed.

NO.	WEEK / ACTIVITY	1	2	3	4	5	6	7		8	9	10	11	12	13	14
1.	Preliminary Research Work															
2.	Literature Review															
3.	Study of Particle Imaging Velocimetry Technique															
4.	Experiment Planning															
5.	Fabrication of Mounting Support															
6.	Image Acquisition															

Figure 3.1 Project time line for final year project 1

NO.	WEEK / ACTIVITY	1	2	3	4	5	6	7		8	9	10	11	12	13	14
1.	Image Acquisition															
2.	Image Processing															
3.	Data Analysis and Interpretation															
4.	Report Writing															
5.	Submission of Technical Paper															
6.	Oral Presentation															
7.	Submission of Report															

Figure 3.2 Project time line for final year project 2

Before the experiment takes place, the methodology flow chart shown in Figure 3.3 is followed. Study was done to choose the suitable velocimetry technique in order to measure the particle velocity and detailed planning of the experiment was carried out to determine the procedures in conducting the experiment and to identify the parameters which will be studied. Followed by is the set-up of the equipments and the steps required to execute the PIV. Finally, the result obtained will be analyzed to extract the trajectories and velocity of the particles.

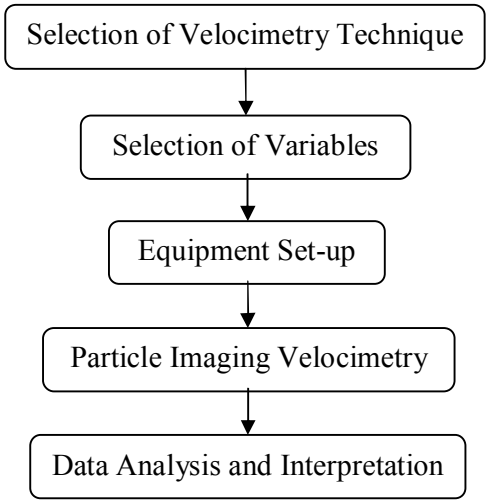

Figure 3.3 Flow chart of methodology

3.1 Selection of Velocimetry Technique

Velocimetry is defined as the measurement of the velocity of fluids. There are varies methods of velocimetry which include Laser-Doppler Velocimetry, Pitot, Hot Wire Velocimetry, Laser-Based Interferometry, Molecular Tagging etc. With the advanced development of computer vision and image processing, optical techniques have rapidly gained their recognition globally as the most advanced flow velocimetry techniques due to their ability in providing precise, instantaneous and quantitative analysis of two-or-three dimensional complex flow fields and two-phase fluid flows. The optical techniques are multi-point methods since they give information wherever particle images are found while Laser-Doppler Velocimetry, Pitot, Hot Wire Velocimetry etc. use single point methods meaning they provide the time history of

velocity only in a single point of space. Thus, optical techniques are much preferred in most of the fluid flow studies.

Optical techniques basically can be divided into two classifications: Particle Imaging Velocimetry and Particle Tracking Velocimetry. PIV and PTV are basically having the same procedures of measuring. However, they have different natural fields of application due to their different ways of working. PIV implies a spectral analysis of a group of particles images, lying on an interrogation area (Adrian, 1991) while PTV involves the identification and location of each particle image in order to recognize its trajectory. In other words, PTV determines the Lagrangian velocity of the particles whereas PIV provides Eulerian description of the particles.

In this project, PIV is selected as the measuring method due to its less complicated algorithm and it is remarkably noise-tolerant and robust in comparison to PTV. The fluid flow is visualized by seeded particles or dye materials and their motion in the whole flow field can be measured from a series of consecutive images in order to recognize its trajectory and to derive the velocity vector field. In other words, PIV provides Eulerian description of the particles and the average displacements of many images inside a certain small interrogation.

PIV offers many advantages for the study of fluid flow due to its merits such as instantaneous whole flow field measurement, contact-free measurement, easy extraction and processing of physical information through velocity information (Yamamoto et al, 1994). However, the main challenge is particle identification because of the appearing and disappearing of particles and ambiguity due to the presence of more than one particle in the neighbourhood. Furthermore, when there are vast amounts of images taken, processing and analysis may become difficult to be handled.

According to Prasad (2000), there are basically four components required in PIV: (1) An optically transparent test-section containing the flow seeded with tracer particles; (2) A light source to illuminate the region of interest (plane or volume); (3) Recording hardware such as camera; (4) A computer with suitable software to

process the images and extract the velocity information. Nevertheless, a number of options are available to create a new PIV system depended on simplicity, cost and the nature of the experiment.

3.2 Selection of Parameters

To investigate the particle motion of the particles, several parameters are chosen to study their effects on the particle velocity. The parameters include blade angle, particle size, particle shape, superficial velocity (air velocity) and bed weight. Table 3.1 shows the parameters set for the experiment.

Table 3.1 Parameters of experiment

Parameter	Description
Blade angle	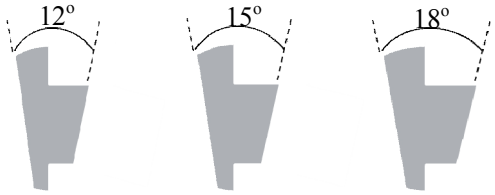
Particle Size	 D = 2900 μm Mass = 11.30 mg D = 3900 μm Mass = 23.69 mg
Particle Shape	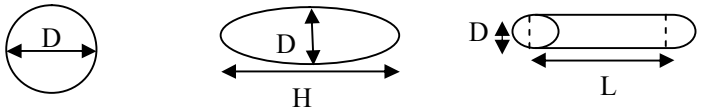 Spherical D = 3900 μm Mass = 23.7 mg Spheroidal D = 3000 μm H = 5900 μm Mass = 24.7 mg Cylindrical D = 1900 μm L = 6400 μm Mass = 35.08 mg
Superficial Velocity (Air Velocity)	Velocity range in steady state swirling regime of operation and early bubbling regime of operation
Bed Weight	500 g, 750 g, 1000 g, 1250 g, 1500 g

Blade angles of 12°, 15° and 18° were manufactured and compared in this study. Two different sizes of sphere PVC particle (3900 μm and 2900 μm) were selected for the investigation of the effect of particle size. Spherical, spheroidal (rice-shaped) and cylindrical particles were chosen for particle shape comparison as they were commonly used in the applications of fluidized bed such as catalyst, medicine pill, biomass briquettes etc. Superficial velocity of the air entering the bed was adjusted within the range of producing stable swirling regime of operation and the bed weight varied from 500 g to 1500 g with increment of 250 g, were used. The experiment conditions were summarized in Table 3.2.

Table 3.2 Experiment conditions

		Blade Angle	**Particle Size**	**Particle Shape**	**Bed Weight**
Blade Angle	**12°**		3900 μm	Spherical	500 g
	15°				
	18°				
Particle Size	**2900 μm**	15°		Spherical	500 g – 1500 g
	3900 μm				
Particle Shape	**Spherical**	15°	*Refer to Table 3.1*		500g – 1500 g
	Spheroidal				
	Cylindrical				
Bed Weight	**500 g**	15°	3900 μm	Spherical	
	750 g				
	1000 g				
	1250 g				
	1500 g				

** Superficial Velocity is set according to the range when stable swirling regime of operation occurs.*

3.3 Equipment Set-up

To conduct the experiment, a pilot scale swirling fluidized bed with an annular blade distributor was set up. Sixty blades were arranged on the outer and inner aluminium holders with a hollow mental cone placed in the centre of the bed. A 30 cm diameter of Plexiglass bed column was fixed on the bed with bolts and nuts. A 5.5 kW high pressure blower with a maximum static pressure of 600 mm w.g. and flow rate of 1000 m^3/hr was connected to the windbox at the bottom of the fluidized bed through a 10 cm diameter pipe with an orifice plate located in the middle of the

pipeline to measure the pressure of the air flow. The pressure recorded was used to calculate the superficial velocity of the air entering the distributor.

In setting the Particle Imaging Velocimetry (PIV) system, a high-speed camera, a halogen lamp, mounting support and computer were required. The high speed camera used was Phantom® ir300 manufactured by Vision Research Inc. as shown in Figure 3.4 and the specifications of the camera is summarized in Table 3.3.

Figure 3.4 Image of the high speed camera

Table 3.3 Specifications of the high speed camera

Maximum Frame Rate	6688fps at full revolution
Maximum Resolution	2048 x 2048
Sensor	Extended-range CMOS sensor
Image Depth	14-bit

The mounting support which allowed imaging from the top of the bed for the camera was custom-made. The reason was that the available tripod could not be utilized due to the height of the bed which was approximately 160 cm and the direction of the camera view was from the top of the bed. The computer used for this application was a laptop due to its mobility and light-weight. Figure 3.5 illustrates the configuration of the whole equipment set up including the SFB and the PIV while Figure 3.6 shows the dimensions of the SFB.

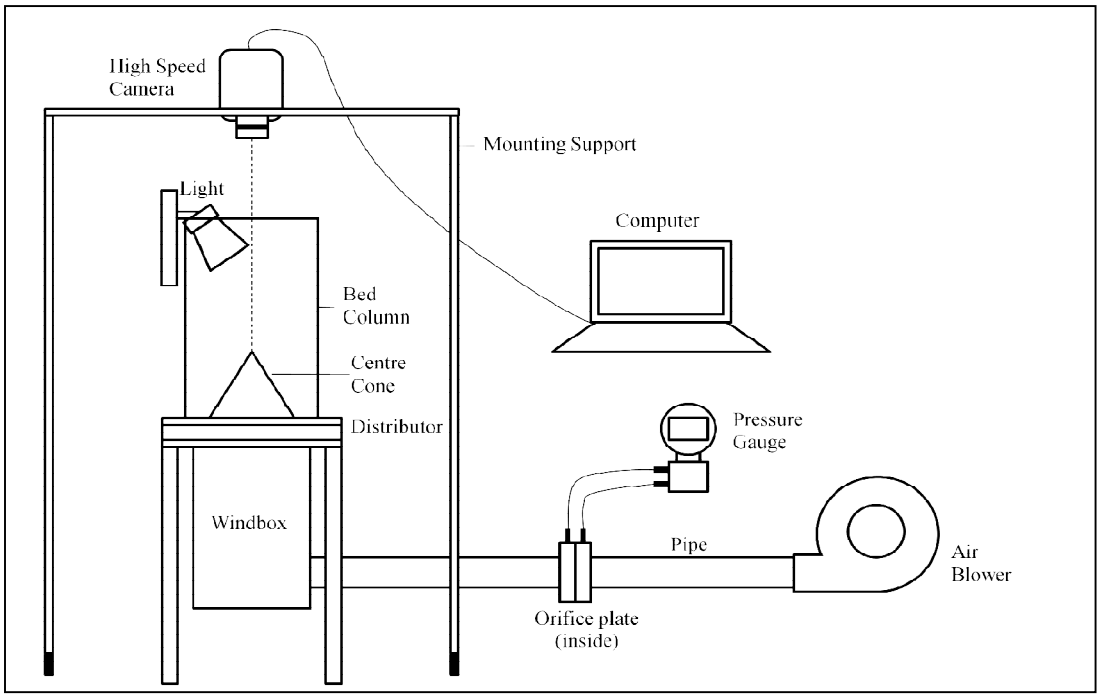

Figure 3.5 Schematic of the pilot scale swirling fluidized bed with particle imaging velocimetry

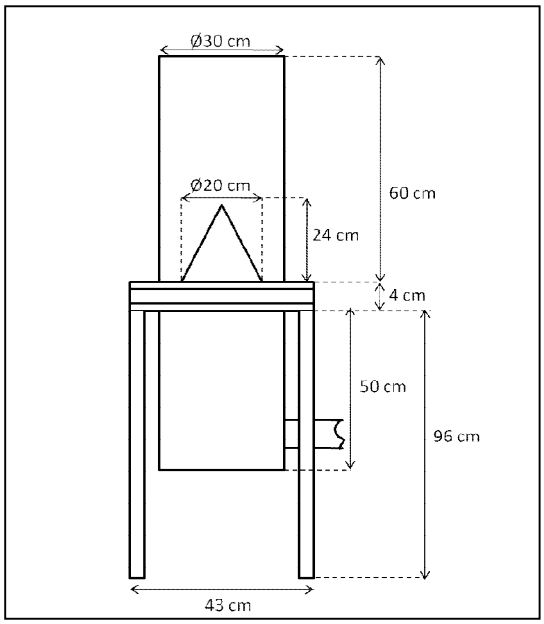

Figure 3.6 Dimensions of swirling fluidized bed

3.4 Particle Imaging Velocimetry

The working scheme of PIV can basically be broken down into four phases which are seeding, illuminating, photographing and image processing as shown in Figure 3.7. Each of these phases will be further discussed in next sections with relation to the experiment of this project.

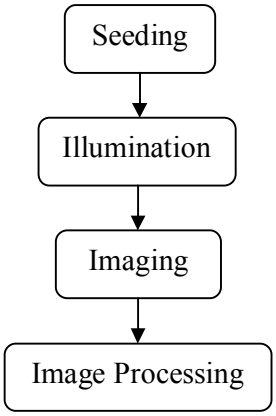

Figure 3.7 Working scheme of particle imaging velocimetry

3.4.1 Seeding

The particles flowing in the fluidized was in very high density which increases difficulty in identifying the tracer particles. To distinguish the tracer particles from the flowing particles, a mixture of black and white as well as blue and white particles were used rather than particles of just one colour. The white particles gave good light reflection to the camera which enabled them to be the tracer particles in this experiment. Different mixture ratios of coloured particles were tested and Table 3.4 shows the final ratios used for each particle shape and size.

Table 3.4 Colours and ratios of the particles used

Particle	Colour	Ratio
Big Spherical (3900 μm)	White (Tracer) : Blue	1:4
Small Spherical (2900 μm)	White (Tracer) : Blue	2:3
Spheroidal	White (Tracer) : Black	2:3
Cylindrical	White (Tracer) : Blue	2:3

3.4.2 Illumination

Generally, PIV uses laser sheeting perpendicular to the imaging direction or a fluorescent illumination behind the measured area for the illumination purpose. However, in this experiment both of these lighting methods could not be applied since this system was opaque and observations were limited to the top layers of the bed. It was impossible to create the laser sheet from the side or to create an illumination which covers the whole bed area using backlight illumination. Another issue when using top illumination was that the position of the light source. The lamp blocked part of the camera view when it was placed below the camera. Even if it was placed above the camera, the intensity of the light weakened and shadow of the camera itself could be seen in the image. Thus, only images of a quarter of the bed were taken. The circular motion of the particles was assumed to be the same no matter where the section was chosen because it was a circle. With that, a halogen lamp was used to illuminate the section from the top opposite of the bed section with angle adjusted as shown in Figure 3.8, to give the best illumination.

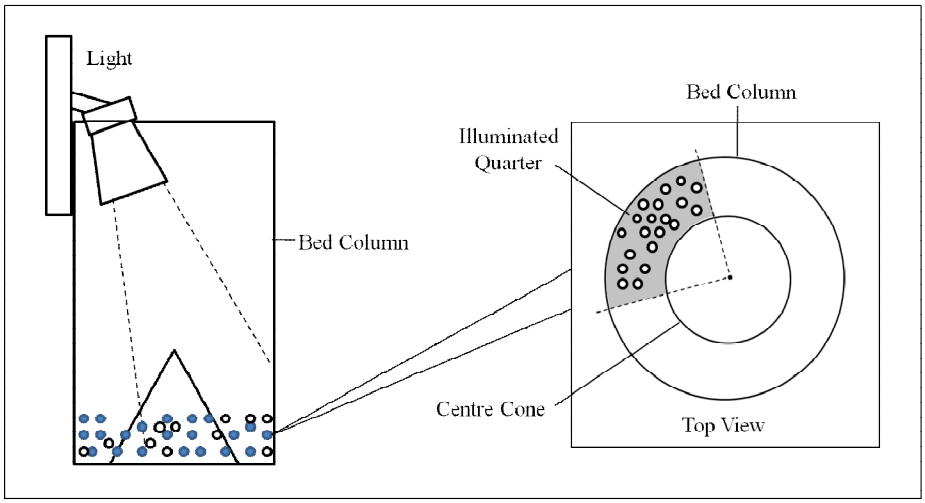

Figure 3.8 Illumination system for swirling fluidized bed

3.4.3 Imaging

After seeding the flow and adjusting the light angle, images of the flow were recorded by the high speed camera. The optical axis of the camera lens must be perpendicular to the plane but it was not easy to set up the camera precisely.

Therefore, calibration needed to be done to determine the parameters every time before taking image. The camera lens was adjusted until a clear image was obtained. Suitable resolution was set and in this case was 864 x 856 pixels then a static image of the whole bed without any movement of the flow was taken. The known dimensions such as the diameter of the bed column and the diameter of the centre cone in the image were used to give the real scale or coordinate for the calculation of displacement and velocity in image processing. Exposure time (430 μs to 990 μs) and frame rate (1200 pps to 2200 pps) were adjusted in order to match with the illumination condition and the particle velocity.

3.4.4 Image Processing

Image processing is the most important stage in PIV. In this experiment, Binary Image Cross-Correlation Method (BICC) was used for the measurement of displacement and velocity. According to Abdulmouti and Mansour (2006), this method employed an algorithm of particle distribution pattern tracking. The motion of each tracer particle was tracked based on the highest similarity of particle distribution patterns in two-consecutive images. The pattern was used for pattern matching and which will give information about the displacement. Then the displacement could be divided by the time interval (from frame rate) and the velocity was obtained. In order to execute image processing, Matlab software was used and program including several steps as shown in Figure 3.9 were developed.

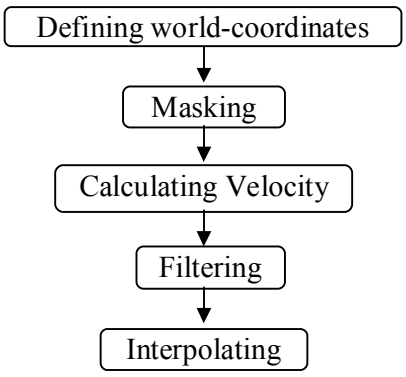

Figure 3.9 Steps taken in image processing

First, “world-coordinates” had to be defined. This was to determine how big a pixel in the image was or in other words, it was a process to transform the local camera coordinates (pixels) to the real physical world coordinate of the experiment by using the dimensions known in the static image as discussed in Section 3.4.4.

The “unwanted” area with no velocity was masked out so that no calculation would be done on that region. With that, calculation of velocity was started. To calculate the velocity of the tracer particles, the image was subdivided into smaller regions called interrogation-windows. The interrogation windows could be of 64 x 64 pixels, 32 x 32 pixels or 16 x 16 pixels. In this experiment, 32 x 32 pixels of interrogation window was used to suit the number of particles. The particles pattern in a sub-window in the first image with the corresponding sub-window in the second image was compared and this comparison continues to the following interrogation windows till it ended. However, it was necessary to eliminate some “unusual” velocities in the image.

Thus, in the next step, filtering was to be done. There are basically three filters used which were signal-to-noise ratio filter, global filter and local filter. Signal-to noise ratio filter used information available in the correlation plane to quantify if the signal strength was "high" compared to the noise level. The global filter removed velocities which were larger than a set threshold times the standard deviation of the measured-velocity field while local filter excluded vectors which were having much difference with the neighbouring interrogation windows. Since some vectors had been eliminated by filters, there were holes left in the velocity field. These holes could be filled by interpolation from the existing data such as the neighbouring velocity near the holes. Finally, a complete velocity field was obtained.

CHAPTER 4

RESULTS AND DISCUSSSIONS

4.1 Data Gathering

A total of 1345 sets of images had been taken. Good quality images were chosen to be processed and five repetitions had been carried out to increase the accuracy of the measurement. Figure 4.1 shows the particles motion for one of the experiments which is 2900 μm diameter sphere particles of 750 g with 58 mm H_2O pressure drop across the orifice plate and time interval of 0.016 s.

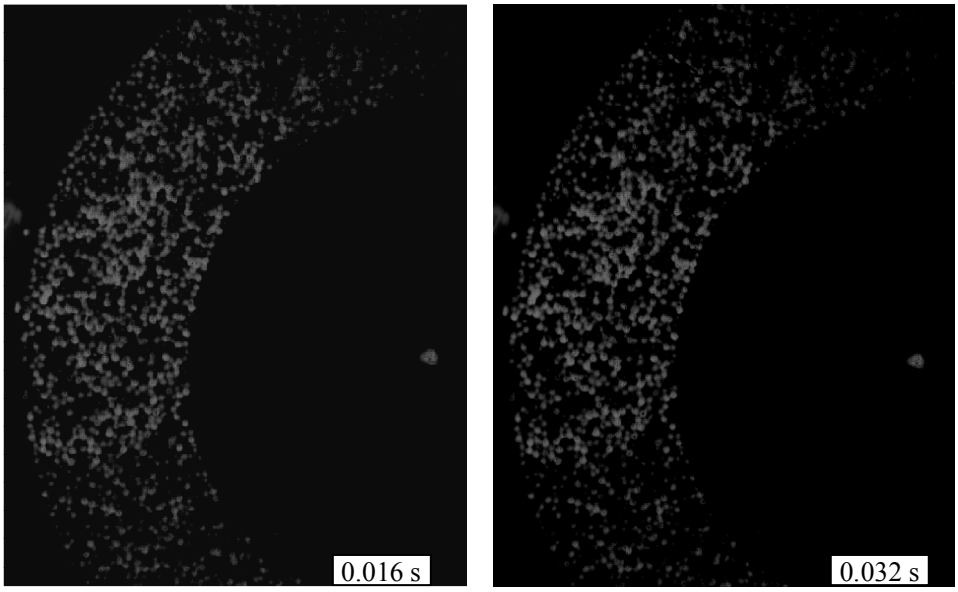

Figure 4.1 Particle motion of 2900 μm diameter sphere particles of 750 g with 58 mm H_2O pressure drop.

4.2 Data Analysis

Before images were analyzed, superficial velocity or air jet velocity is determined from the equations as discussed in Section 4.2.1. Graphs were plotted from the velocity fields obtained from PIV and were presented according to different parameters concerned such as blade angle, particle size and particle shape.

4.2.1 Superficial Velocity

In order to calculate superficial velocity entering the bed, the air flow rate through the pipe had to be determined from the pressure drop in the orifice plate. Equation 4.1 was used to calculate the air flow rate referring to the dimensions of orifice plate as shown in Figure 4.2.

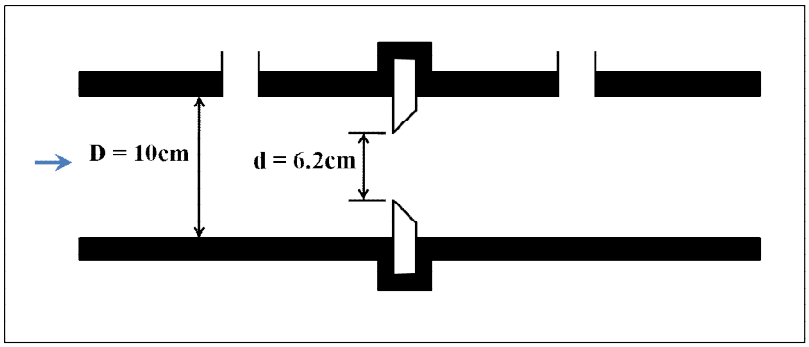

Figure 4.2 Dimensions of the orifice plate

$$\dot{Q} = A_0 C_d \sqrt{\frac{2(P_1 - P_2)}{\rho(1-\beta^4)}} \qquad (4.1)$$

where $\dot{Q}$ is the air flow rate through the pipe, A_0 is the cross-sectional area of the hole, C_d is a constant which depends on the particular design of the orifice plate, $P_1 - P_2$ is the pressure drop which was recorded from the pressure gauge, ρ is the air density which was assumed to be 1.2 kg/ m^3 and β is the diameter ratio d/D. In this case, the C_d is 0.668. Having the air flow rate, superficial velocity, $V_{superficial}$ was calculated by dividing the air flow rate, $\dot{Q}$ with bed area, A_{bed}:.

$$V_{superficial} = \frac{\dot{Q}}{A_{bed}} = \frac{\dot{Q}}{\frac{\pi}{4}(D_o{}^2 - D_i{}^2)} \qquad (4.2)$$

The diameter of the bed column, D_o is 30cm while the diameter of the centre cone, D_i is 20 cm.

4.2.2 Velocity Field Interpretation

Velocity fields were generated from the PIV program and five particle velocities were averaged to obtain final velocity. Figure 4.3 illustrates one of the velocity fields gained for the 750 g bed weight of 2900 µm spherical particles at 2 m/s of air superficial velocity. The velocity field shows the particle trajectory and the colour bar indicates velocity in m/s unit.

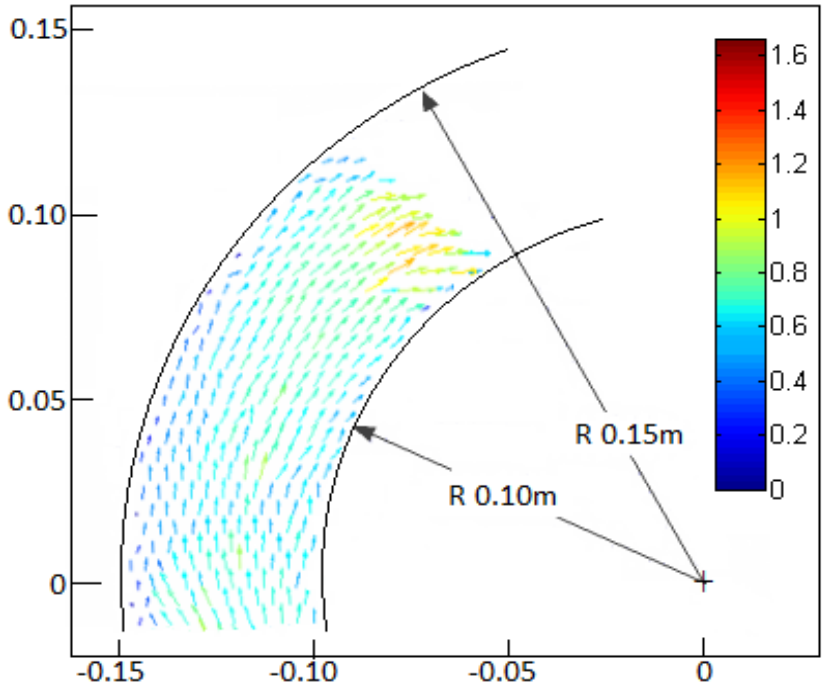

Figure 4.3 Typical velocity field of particles, dimension in meter

From the velocity field, velocity profiles at every 15^{o} angle were drawn as shown in Figure 4.4. It could be observed that the particles which were about to turn at the corner (uppermost velocity profile) had higher velocity whereas the particles before the corner were moving at similar velocity. Thus, the intermediate velocity profile just before the corner was selected to be measured. Shown in Figure 4.5 is the selected velocity and the average velocity of the particles was calculated from the equivalent velocity area obtained from the velocity profile.

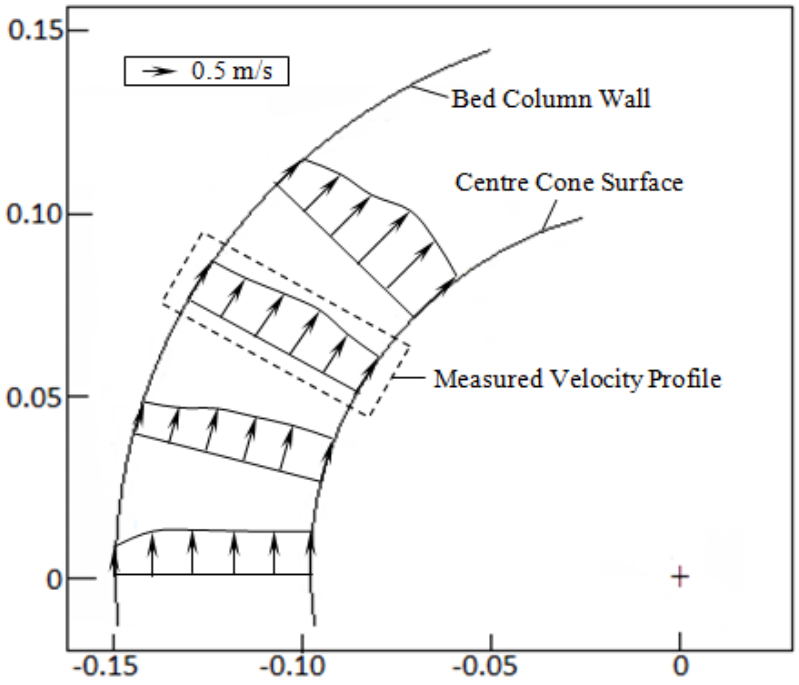

Figure 4.4 Velocity profiles at different locations

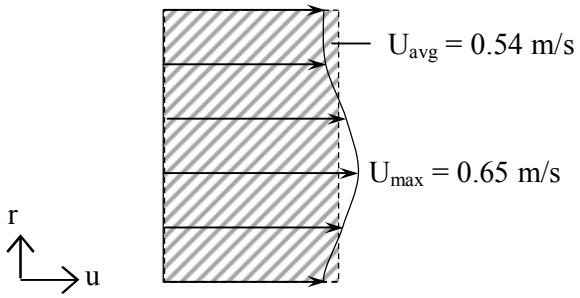

Figure 4.5 Average particle velocity

However, depending on the air superficial velocity, different pattern of velocity profile could be obtained. Table 4.1 shows the velocity profile of 2900 μm spherical particles at 750 g bed weight with increasing air superficial velocity. At low superficial velocity, particles near bed column wall and centre cone were slowed down by friction. Particles which contacted with centre cone surface possessed lowest velocity while particles in the middle region had highest velocity. As superficial velocity increased, the velocity near surfaces started to increase as the swirling momentum of particles was sufficient to overcome the friction. The velocity

of particles near centre cone developed with superficial velocity and was getting higher. The velocity of particles which was in contact with bed column wall, remained at low value regardless of increasing superficial velocity. This was due to the centrifugal force which had increased with superficial velocity. Strong centrifugal force pushed the particles towards bed column wall, which increased the inter-particle friction and surface friction. However, this centrifugal force had reduced friction on the inner radius particles, which enabled the particles to swirl at highest velocity.

Table 4.1 Velocity profile with increasing air superficial velocity

Air Superficial Velocity (m/s)	Velocity Profile	Average Particle Velocity (m/s)
1.60	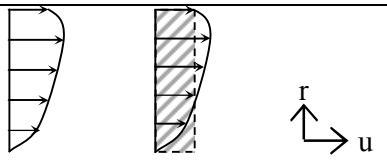	0.72
1.75	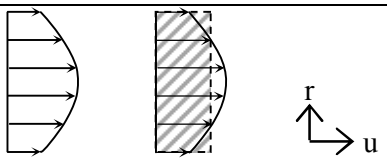	0.80
1.90	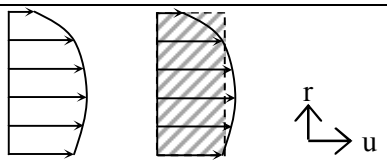	0.83
2.02	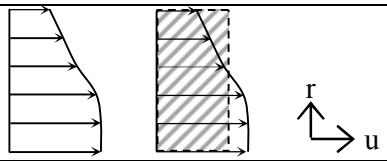	0.84
2.14	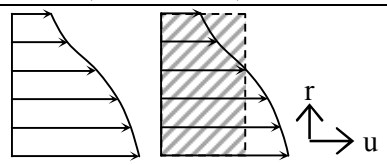	0.92

4.2.3 Effect of Bed Weight

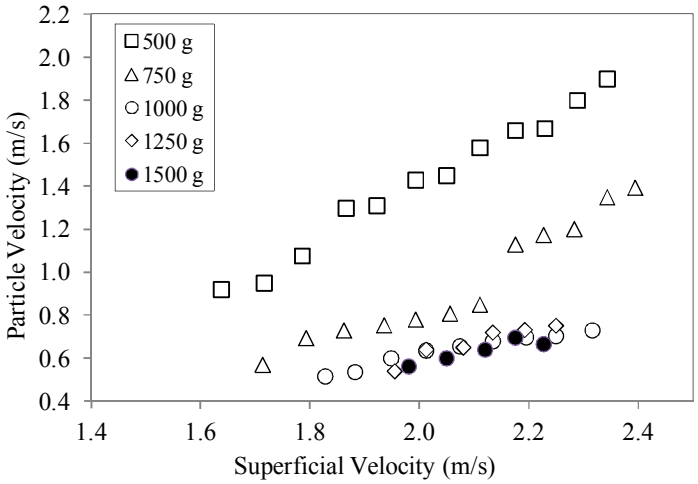

Figure 4.6 Variation of particle velocity for different bed weight of spherical particles

Figure 4.6 shows the variation of 3900 μm sphere particle velocity with air superficial velocity at different bed weight which was varied from 500 g to 1500 g at an increment of 250 g. It is shown that particle velocity decreases with bed weight. This was due to bed height, which was synonymous with bed weight and it was noted that the observed particle velocity in the bed pertained to the uppermost layer of the bed. As the jet air percolated through the bed, its velocity continuously decreased due to the transfer of momentum to the particles. Correspondingly, the particle velocity in the uppermost layer decayed as the bed height increased.

When bed weight was increased, the particle velocity was less sensitive to the change of superficial velocity. This can be observed from the graph that the range of particle velocity of 500 g bed weight is largest and the range becomes smaller with increasing bed weight. Besides, minimum swirling superficial velocity increased with bed weight. The reason for these trends was heavier bed weight had larger amount of particles which resulted in higher friction between the particles as well as wall friction. This reduced the swirling momentum from the jet air.

Another observation was that over 1000 g bed weight, the particle velocity remained almost constant regardless of the increasing bed weight. It was found that the

particles were actually moved by the expansion of bubbles. These bubbles formed were not vigorous and random. Instead, their occurrences were consistent and less dynamic, which gave a constant velocity trend to the particle.

4.2.4 Effect of Blade Angle

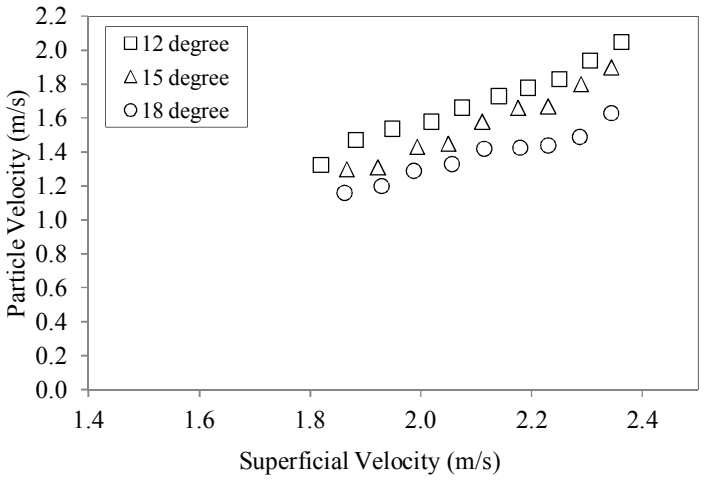

Figure 4.7 Variation of particle velocity for different blade angles

Figure 4.7 shows the variation of particle velocity with air superficial velocity at blade angle of 12^{o}, 15^{o} and 18^{o}. It was observed that there was a large gap before 1.8 m/s of air superficial velocity, which should be noted that it was the range where bubbling and slugging regime occurred before stable swirling was achieved. It is obvious that the particle velocity increased as air superficial velocity was increased but it decreased as the blade angle was increased. A plausible explanation for this was that larger blade angle gave higher friction to the particle due to its larger contact surface area with the particles. From the analysis, it was concluded that 3^{o} increment of blade angle brought reduction of less than 18% on particle velocity.

4.2.5 Effect of Particle Size

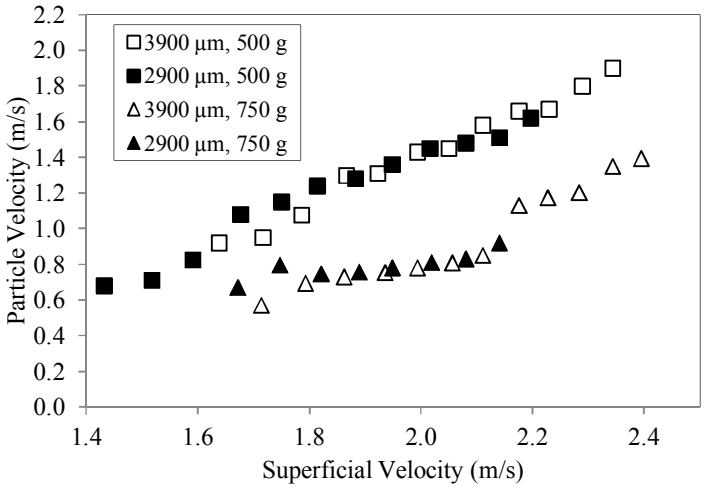

Figure 4.8 Variation of particle velocity for different spherical particle sizes

Shown in Figure 4.8 is the velocity variation of 3900 µm and 2900 µm spherical particles, with air superficial velocity at bed weights of 500 g and 750 g. Only two bed weights were available for comparison and this was mainly due to the smaller 2900 µm spherical particles which had no stable swirling regime of operation but dynamic bubbling top layer when the bed weight exceeded 750 g.

Overall, the particle velocity of both sizes of particles increased with air superficial velocity. It was found that 2900 µm spherical particles had lower minimum swirling air superficial velocity than 3900 µm spherical particles. The smaller spherical particles started to swirl when air superficial velocity was approximately 1.3 m/s while the larger spherical particles reached stable swirling at 1.6 m/s for 500 g bed weight. This implied that stable swirling regime of operation in the smaller particle also ended earlier and thus the operating regime of superficial velocity was shifted down. Thus, it was proposed that smaller particle size is preferred for applications of shallow bed with the reason that lower air superficial velocity is sufficient to start swirling the particles as compared to bigger particles. In other words, less energy is needed to swirl small particles.

4.2.6 Effect of Particle Shape

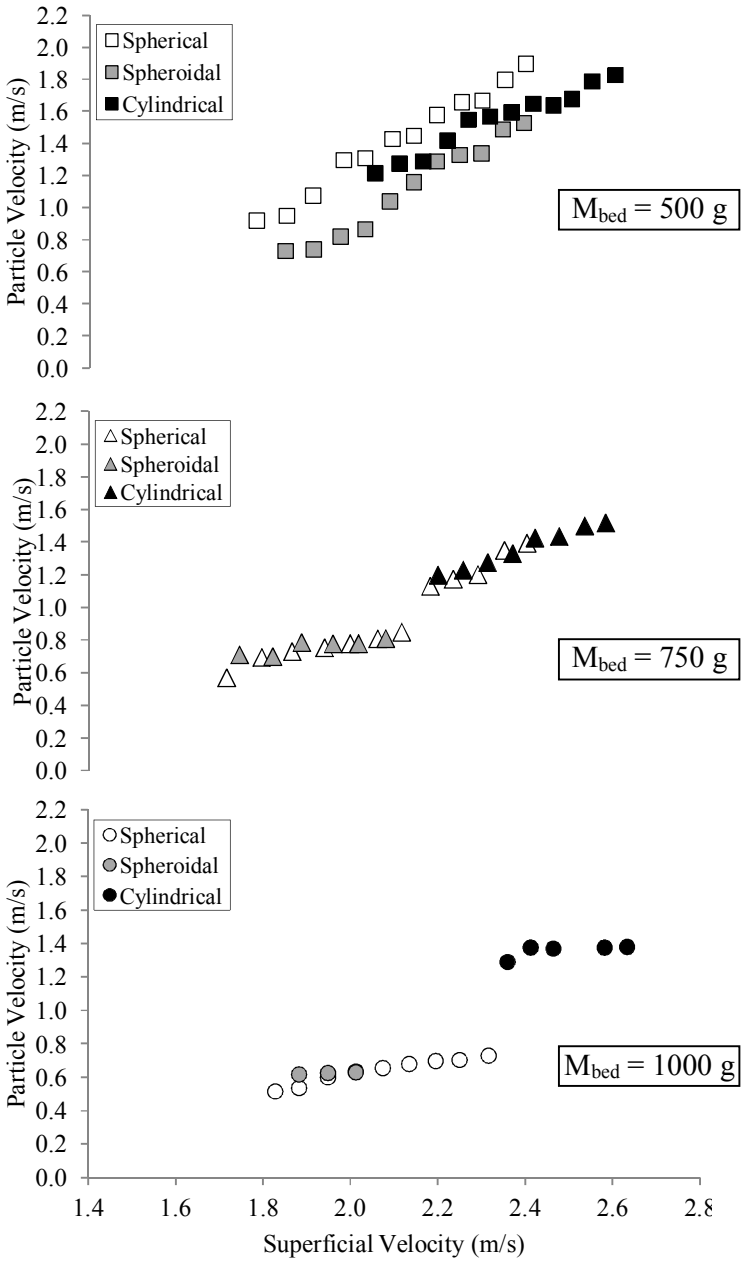

Figure 4.9 Variation of particle velocity for different particle shape

Shown in Figure 4.9 are the changes of spherical, spheroidal and cylindrical particles as a result of air superficial velocity at bed weight between 500 g to 1000 g. From the observation, the particle velocity of all shapes increased with air superficial velocity

but when the bed weight was increased, the variation of the particle velocity reduced and this was due to the occurrence of constant bubbling described earlier in the bed weight discussion.

Both spherical and spheroidal particles start swirling at similar air superficial velocity. However, the velocity for spheroidal particles was smaller than spherical particles. This was because larger surface area of spheroidal particle created more inter-friction which reduced the particle velocity. However, this trend did not apply to heavier bed weight such as 750 g and 1000 g as the particle velocity of the both shapes of particle were overlapping and it was because of bubbling.

For 750 g and 1000 g bed weight, spheroidal particles had very short stable swirling range due to vigorous bubbling layer. This showed that spheroidal particle were prone to be elevated easily due to its larger surface area parallel to the bed which enabled more jet air be injected on it and more vertical motion was produced. It should be noted that this narrow swirling range did not happen to cylindrical particles which had larger surface area than the spheroidal particles because the cylindrical particles did not show shorter swirling range. The explanation for this was the cylindrical particles were heavier thus elevation which causes bubbling, was not as easy as spheroidal particles.

Cylindrical particles showed higher minimum swirling air superficial velocity which shifted up the stable swirling range. This was also due to its heavier mass which possessed larger inertia and required higher momentum of air to move. With increasing bed weight, the velocity gap between cylindrical particles and the other two shapes of particles was getting wider. This indicated that the velocity of cylindrical particles did not reduced as much as spherical and spheroidal particles. The velocity of the spherical and spheroidal reduced much because of their deep bed height which attenuated the jet air momentum transferred to the top layer particles. Cylindrical particles did not encounter deep bed because its heavier particle mass enabled less particles needed to reach the same bed weight as the spherical and

spheroidal particles, thus resulted in shallower bed. Therefore, momentum of jet air could still be able to be transferred to the top layer particles efficiently.

It could be concluded that spherical particle was preferred for application as it provided broader stable swirling regime and lower minimum swirling air superficial velocity which means higher efficiency and less energy requirement. Larger surface area parallel to the bed bottom gave spheroidal particles narrow stable swirling range due to bubbling. This could be remedied by heavier particles as shown by cylindrical particle but larger minimum swirling air superficial velocity was required.

CHAPTER 5

CONCLUSIONS AND RECOMMENDATIONS

Particle motion and the effects of several operating parameters such as air superficial velocity, bed weight, blade angle, particle size and particle shape, on the particle velocity in a pilot scale SFB have been studied by using modified PIV technique. Particle trajectories and velocity are obtained from the velocity field generated from the PIV technique, which enable analysis of the graphs for different operating parameters studied. From the analysis which has been done, following conclusions were obtained:

- The decrease of particle velocity in response to increasing bed weight and reduction of superficial velocity were in conformity with theories. An interesting finding was that when bed weight was increased, the particle velocity was less sensitive to the increase of superficial velocity.

- Particle velocity increased when the blade angle decreased and small change of 3^{o} in blade angle yielded less than 18% variation on particle velocity.

- Smaller size of particle required lower air superficial velocity for stable swirling but with constraint of shallow bed.

- Spherical particles possessed broader stable swirling regime range and required lower swirling air superficial velocity whereas spheroidal particles gave narrower stable swirling range due to bubbling. However, when heavier cylindrical particles were operated, bubbling was reduced but air superficial velocity was required to swirl the particle.

These findings will contribute to the design of scaled-up commercial SFB unit which has not been fully developed yet due to the lack of study and understanding of the particle dynamic characteristics. The evaluations of the effect resulted from the operating parameters are able to serve as reference for the validation of analytical model of SFB done by other researchers and finally, the particle velocity obtained from this study provides solution to the calculation of slip velocity which is vital in determining and predicting heat transfer efficiency of the bed.

Thus, one of the future researches that can be done is to evaluate the air velocity profile in order to gain more insight into the correlation between the air and the particle velocities which will lead to the slip velocity determination. The particle velocity obtained from the present work was limited to the top surface of the bed in stable swirling regime of operation with only tangential velocities were investigated. Hence, it is recommended that axial and radial particle velocity and other regime of operations such as slugging (wave motion) and bubbling should be studied. Improved technique of PIV and more measurements should be done to obtain higher accuracy of particle velocity.

In a nutshell, SFB promises great potential in replacing conventional fluidized bed in future. Its ability in overcoming many drawbacks of the conventional bed such as bed pressure drop, elutriation, particle size limitation etc. demands more researches to reach its higher sense in industrial development.

REFERENCES

Abdulmouti H. and Mansour T.M., 2006, *The Technique of PIV and Its Applications*, 10th International Congress on Liquid Atomization and Spray Systems, Kyoto Japan, Aug 27–Sept 1.

Adrian R.J., 1991, *Particle-imaging techniques for experimental fluid mechanics*, Annual Review of Fluid Mechanics, vol 23, 261-304

Batcha M.F.M. and Raghavan V.R., 2011, *Experimental Studies on a Swirling Fluidized Bed with Annular Distributor*, Journal of Applied Sciences, 11: 1980-1986.

Chyang C.S. and Lin Y.C., 2002, *A study in the swirling fluidizing pattern*, J.Chem. Eng. Japan, 35: 503-512

Geldart D., 1973, *Types of gas fluidization*, Powder Technology, Vol. 7, 285-292.

Hoomans, B. P. B.; Kuipers, J. A. M.; Salleh, M. A. M.; Stein, M. and Seville J. P. K., 2001, *Experimental Validation of Granular Dynamics Simulations of Gas-Fluidised Beds with Homogenous In-Flow Conditions Using Positron Emission Particle Tracking*, Powder Technology, Vol.116, 166-177.

Horio M, 2011, *Fluidization-Past & Future*, The 13th International Conference on Fluidization-New Paradigm in Fluidization Engineering, Vol.RP6, Article 9.

Howard,J.R.,1989. *Fluidized Bed Technology: Principles and Applications.* Adam Hilger Publication, Bristol, UK.

Kaewklum R., Kuprianov V.I., Douglas P.L., 2009, *Hydrodynamics of air-sand flow in a conical swirling fluidized bed*, Energy Conversion Manage., 50: 2999-3006

Kumar V.V. and Raghavan V.R., 2011, Development of fluidized bed technology – a review, National Postgraduate Conference (NPC), 19-20 Sept,

Lee S.W. and Liu Y., 2004, *The Bed Expansion and Particle Velocity Analysis in the Swirling Fluidized Bed Combustor (SFBC) Cold Model*, The Canadian Journal of Engineering, Volume 82, 1054-1058

Mostoufi, N. and Chaouki, J., 2001, *Local Solid Mixing in Gas-Solid Fluidized Beds*, Powder Technology, Vol.114,.23-31

Ouyang F. and Levenspiel O., 1986, *Spiral Distributor for Fluidized Beds*, Ind. Eng. Chem. Process Des. Dev., Vol. 25, 504

Paulose M.M., 2006, *Hydrodynamic Study of Swirling Fluidized Bed and the Role of Distributor*, Cochin University of Science and Technology, May 2006.

Prasad A.K., 2000, *Particle Image Velocimetry*, Current Science, Vol. 79, No. 1, 10 July 2000, 51-60.

Raghavan V.R., Kind M., Martin H., 2004, *Modeling of the Hydrodynamics of Swirling Fluidized Beds*, 4th European Thermal Sciences Conference 'EUROTHERM" & Heat Exchange Engineering Exhibition, Birmingham, UK, 29-31 March 2004.

Sceenivasan B. and Raghavan V.R., *Hydrodynamics of a Swirling Fluidized Bed*, Chemical Engineering and Processing, 41, 99-106, 2002.

Shu J., Lakshmanan V.I., and Dodson C.E., 2000, *Hydrodynamics study of a Toroidal Fluidized Bed Reactor*, Chem. Eng. Process., 39:499-506.

Sobrino C., Almendros-Ibanez J.A., Santana D., Vega M. De, 2008, Fluidization of Group B particles with a rotating distributor, Powder Technology 181, 273-280.

Sowards N.K., 1978, *Low pollution incineration of solid waste*, US Patent 40759351978.

Tsuji T., Miyauchi T., Oh S., Tanaka T., 2010, *Simultaneous Measurement of Particle Motion and Temperature in Two-Dimensional Fluidized Bed with Heat Transfer,* Hosokawa Powder Technolody Foundation KONA Powder and Particle Journal No. 28 (2010).

Vikram G., Martin H. and Raghavan V.R., 2003, *The swirling fluidized bed-An advanced hydrodynamics analysis*, 4th National Workshop & Conference on CFD Technology & Revamping of Boilers in India, Bangalore Engineering College, June 3-4, 9-19.

Yamamoto F., Iguchi M., Ohata J., Andrzej S., 1994, *Fundamentals and Applications of Particles-Imaging Velocimetry (Focusing on Binary Image Cross-Correlation Method for 3D PTV)*, Proceedings of Intentional Conferences on Fluids Engineering at Chosun University, Nov. 1-2, Kwangju, Korea, 39-48

APPENDIX A

EXPERIMENT SET-UP

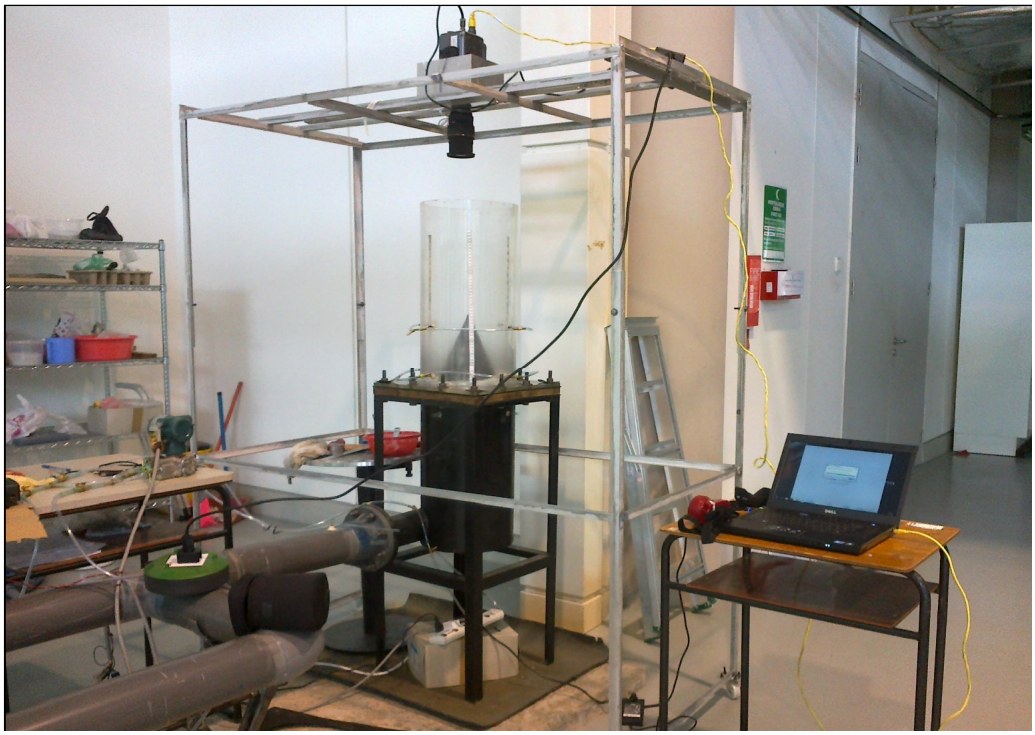

Figure A-1 Experiment set-up

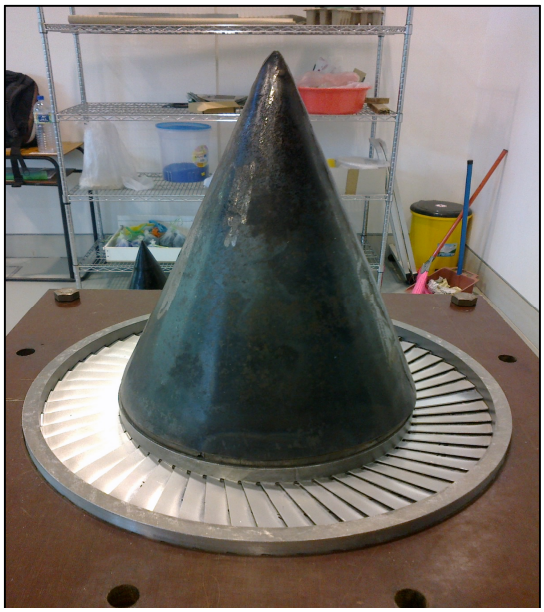

Figure A-2 Centre cone placed in the middle

APPENDIX B

USING PHANTOM CAMERA CONTROL SOFTWARE FOR IMAGE ACQUISITION

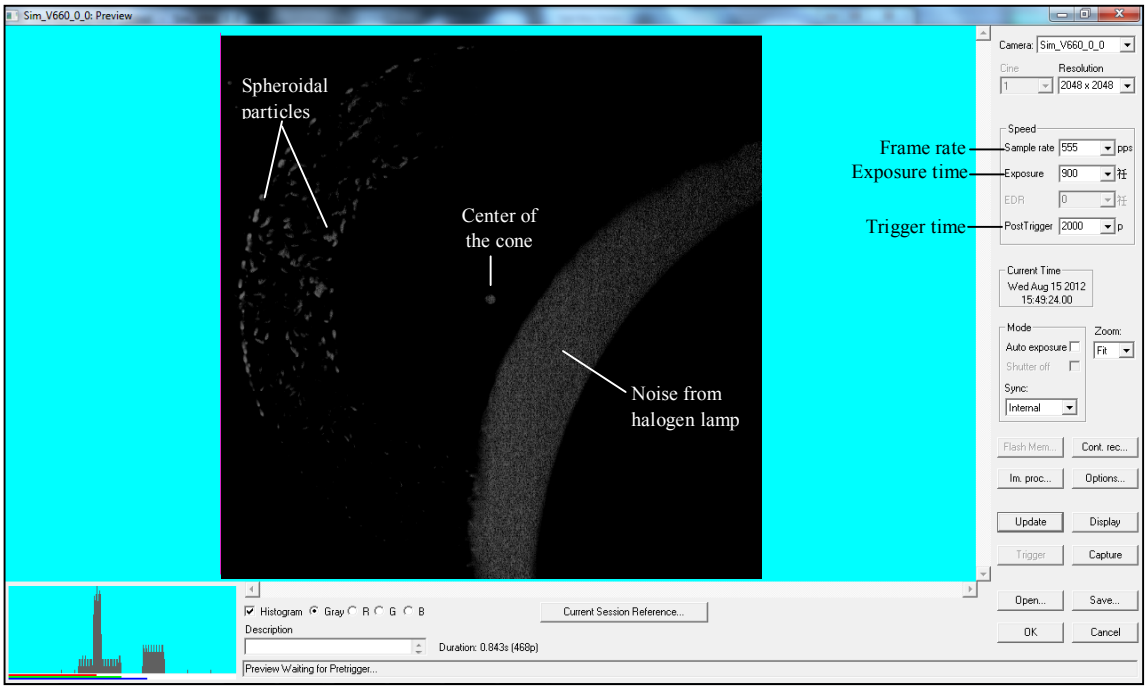

Figure B-1 Acquisition of Image

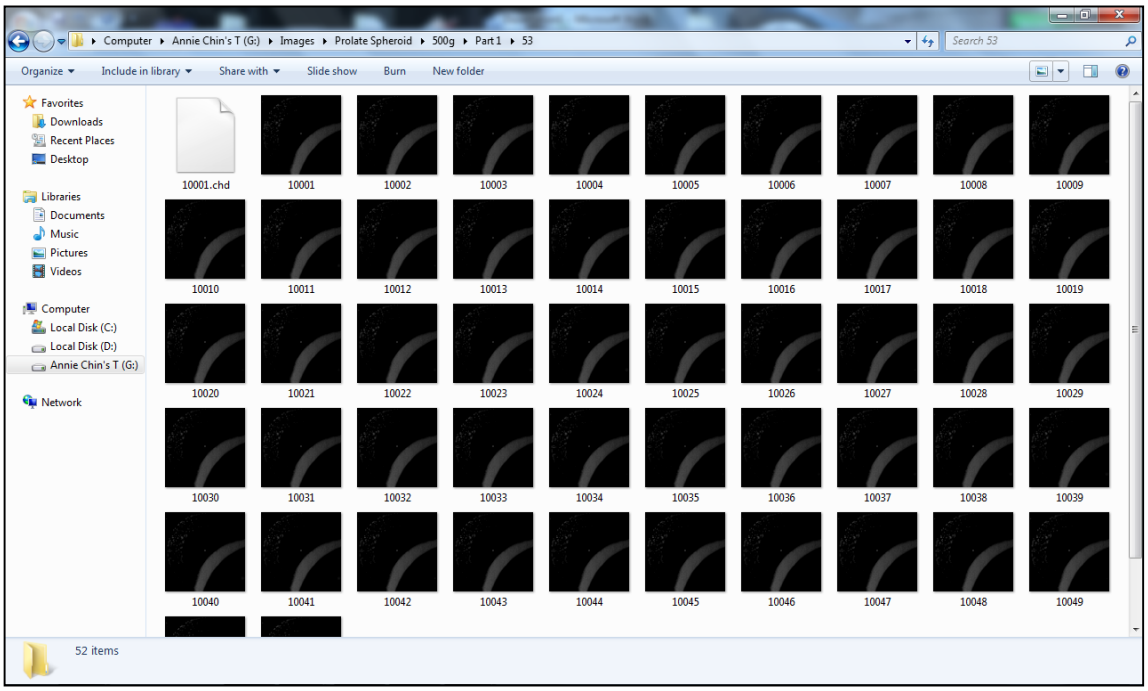

Figure B-2 Saving thousands images

APPENDIX C

USING MATLAB SOFTWARE FOR IMAGE PROCESSING

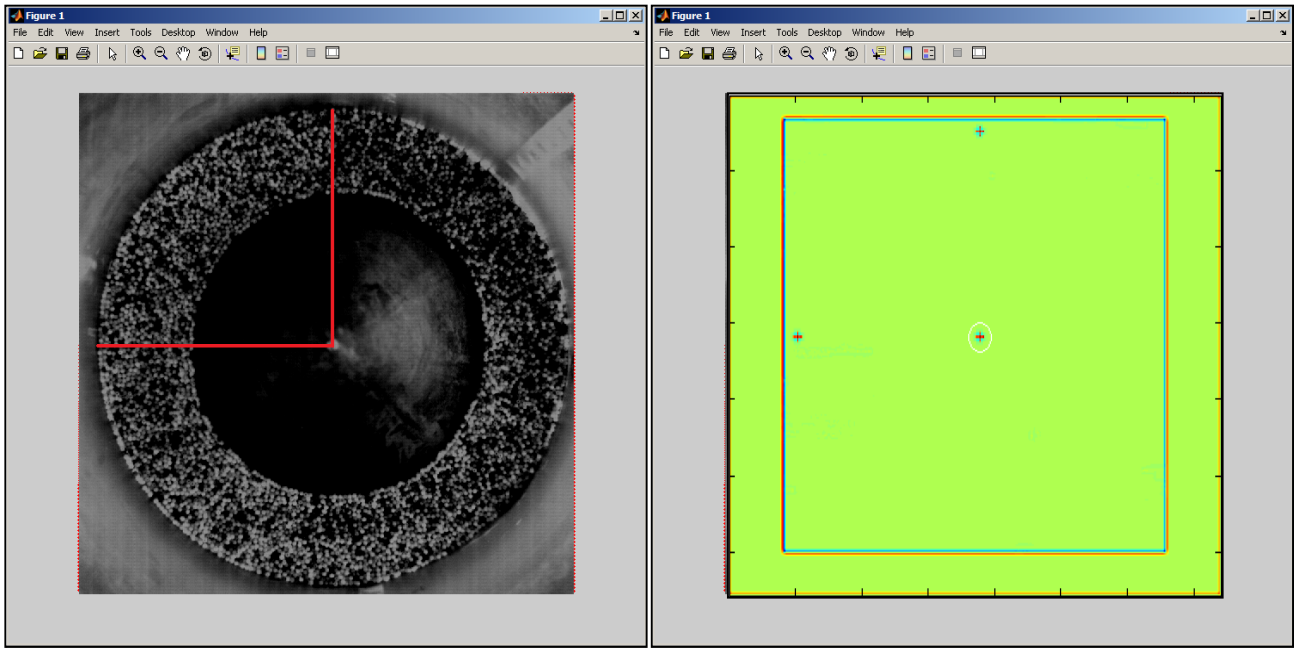

Figure C-1 Identifying “world-coordinate”

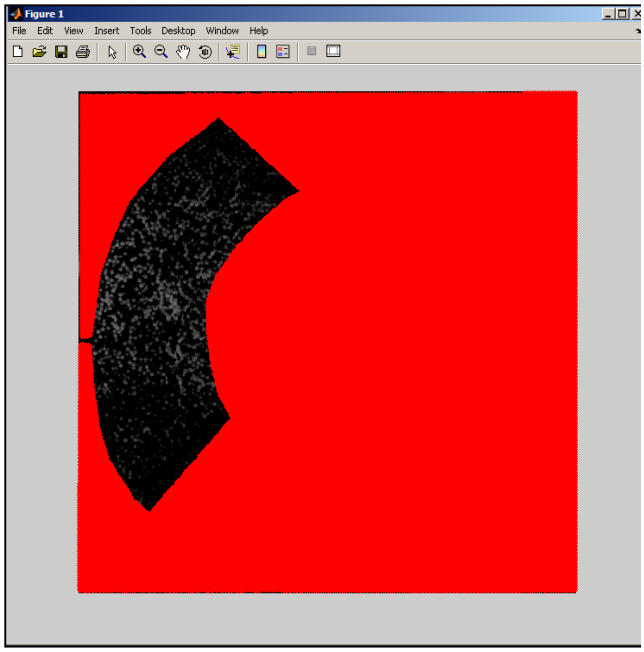

Figure C-2 Masking out “unwanted” area

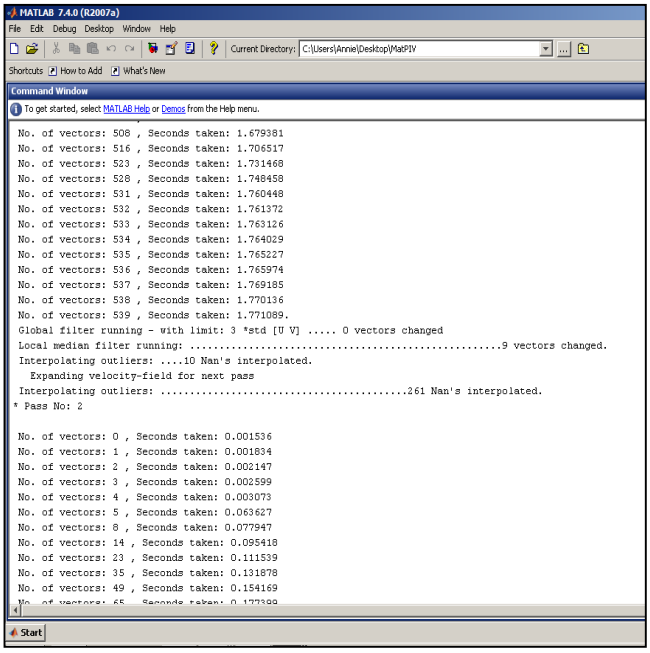

Figure C-3 Filtering and interpolating

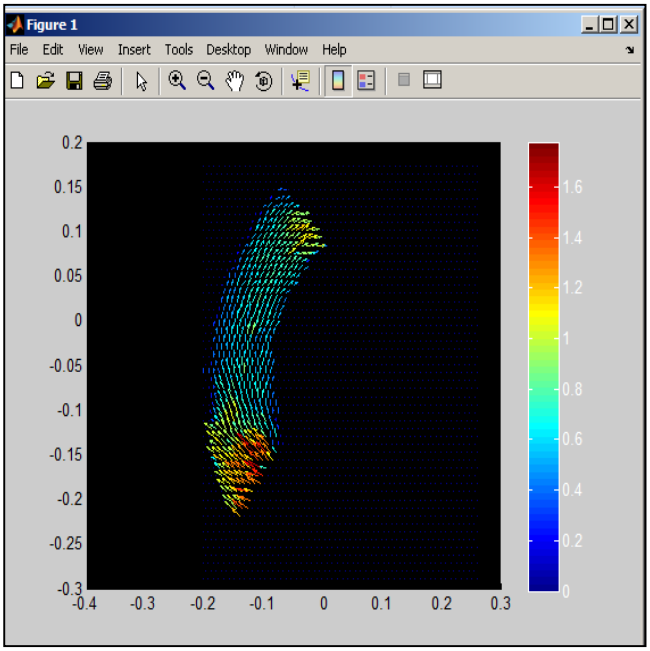

Figure C-4 Velocity field generated

Main Program Code

```
clear all
clc;
fid = fopen('PIV_using_matlab.bin','w');
%%
%%
%%
%
image1 = imread('80.5\10001.tif');
image2 = imread('80.5\10003.tif');
%%%%%%%%%%%%%%%%%%%%%%%%%%%%%%%%%%%%%%%%%%%%%%%%%%%%%%%%%%%%%%%%%%%%%%%%
% CONVERT PIXEL COORDINATE INTO WORLD COORDINATE
%
[comap,A1,world]=definewoco('Worldcornew.png','.');
%
% MASK THE UNWANTED REGION USING THE LEFT MOUSE BUTTON
%
maske = mask('80.5\10001.tif','worldco1.mat');
%
% CALCULATING VELOCITY VECTOR USING CROSS CORRELATION OF TWO IMAGES
%
%
[x,y,u,v,snr,pkh]=matpiv(image1,image2,[32 32],0.0011,0.5,...
'multin','worldco1.mat','polymask5.mat');
%
% FILTERING THE RAW VECTORS
%
[su,sv] = snrfilt(x,y,u,v,snr);
[pu,pv] = peakfilt(x,y,su,sv,pkh,0.5);
[gu,gv] = globfilt(x,y,pu,pv,3);
[mu,mv] = localfilt(x,y,gu,gv,2,'median',3,'polymask5.mat');
[fu,fv] = naninterp(mu,mv,'linear','polymask5.mat',x,y);
figure;
hold on
L=sqrt(fu.^2 + fv.^2);
LL=L(isfinite(L));
% pcolor(x,y,L)
% shading interp
quiverc(x(1:4:end),y(1:4:end),fu(1:4:end),fv(1:4:end),2),colorbar('p
eer',gca,'location','EastOutside'), axis auto
caxis([0, max(LL)]);
colorbar
% ncquiverref(x,y,u,v,units,reftype,refvec,veccol,cont)
LL=L(isfinite(L));

fclose(fid);
```

APPENDIX D

RAW DATA OF PARTICLE VELOCITIES

Blade Angle

12°

ΔP Orifice (mm H_2o)	Superficial Velocity (m/s)	Particle Velocity (m/s)					
65.4	1.8190	1.30	1.30	1.40	1.30	1.30	1.32
70.0	1.8819	1.40	1.40	1.40	1.60	1.50	1.46
75.0	1.9480	1.55	1.55	1.55	1.50	1.55	1.54
80.5	2.0181	1.50	1.58	1.60	1.60	1.55	1.57
85.0	2.0738	1.65	1.67	1.65	1.66	1.67	1.66
90.5	2.1398	1.73	1.71	1.72	1.74	1.75	1.73
95.0	2.1923	1.77	1.80	1.79	1.75	1.79	1.78
100.0	2.2493	1.84	1.82	1.82	1.83	1.84	1.83
105.0	2.3048	1.95	1.89	1.95	1.95	1.96	1.94
110.2	2.3612	2.06	2.06	2.03	2.05	2.05	2.05

15°

ΔP Orifice (mm H_2o)	Superficial Velocity (m/s)	Particle Velocity (m/s)					
68.8	1.8657	1.20	1.19	1.40	1.20	1.50	1.30
73.0	1.9218	1.20	1.40	1.30	1.35	1.30	1.31
78.5	1.9929	1.40	1.50	1.30	1.55	1.40	1.43
83.0	2.0492	1.50	1.40	1.45	1.55	1.35	1.45
88.0	2.1100	1.55	1.60	1.50	1.65	1.60	1.58
93.5	2.1750	1.50	1.65	1.70	1.75	1.70	1.66
98.2	2.2290	1.60	1.70	1.70	1.65	1.70	1.67
103.5	2.2883	1.80	1.90	1.80	1.70	1.80	1.80
108.5	2.3429	1.90	1.85	2.00	1.85	1.90	1.90

18°

ΔP Orifice (mm H_2o)	Superficial Velocity (m/s)	Particle Velocity (m/s)					
68.5	1.8616	1.15	1.15	1.15	1.15	1.20	1.16
73.5	1.9284	1.20	1.20	1.20	1.20	1.20	1.20
78.0	1.9865	1.30	1.25	1.30	1.30	1.30	1.29
83.5	2.0554	1.30	1.30	1.40	1.30	1.35	1.33
88.3	2.1136	1.45	1.40	1.35	1.50	1.40	1.42
93.8	2.1785	1.40	1.45	1.38	1.40	1.50	1.43
98.2	2.2290	1.50	1.45	1.40	1.45	1.40	1.44
103.3	2.2861	1.50	1.45	1.45	1.50	1.55	1.49
108.5	2.3429	1.60	1.65	1.70	1.60	1.60	1.63

Particle Size

3900 μm

- **500 g**

ΔP Orifice (mm H_2o)	Superficial Velocity (m/s)	Particle Velocity (m/s)					
53.0	1.6375	0.80	0.90	1.00	0.90	1.00	0.92
58.2	1.7160	1.00	1.10	0.90	0.90	0.85	0.95
63.0	1.7853	1.15	1.00	1.15	1.18	0.90	1.08
68.8	1.8657	1.20	1.19	1.40	1.20	1.50	1.30
73.0	1.9218	1.20	1.40	1.30	1.35	1.30	1.31
78.5	1.9929	1.40	1.50	1.30	1.55	1.40	1.43
83.0	2.0492	1.50	1.40	1.45	1.55	1.35	1.45
88.0	2.1100	1.55	1.60	1.50	1.65	1.60	1.58
93.5	2.1750	1.50	1.65	1.70	1.75	1.70	1.66
98.2	2.2290	1.60	1.70	1.70	1.65	1.70	1.67
103.5	2.2883	1.80	1.90	1.80	1.70	1.80	1.80
108.5	2.3429	1.90	1.85	2.00	1.85	1.90	1.90

- **750 g**

ΔP Orifice (mm H_2o)	Superficial Velocity (m/s)	Particle Velocity (m/s)					
58.0	1.7130	0.50	0.65	0.55	0.55	0.60	0.57
63.5	1.7924	0.65	0.70	0.72	0.75	0.65	0.69
68.5	1.8616	0.70	0.72	0.70	0.78	0.75	0.73
74.0	1.9349	0.75	0.73	0.75	0.79	0.75	0.75
78.5	1.9929	0.80	0.72	0.78	0.80	0.80	0.78
83.5	2.0554	0.80	0.79	0.81	0.85	0.79	0.81
88.0	2.1100	0.75	0.90	0.85	0.85	0.90	0.85
93.5	2.1750	1.00	1.15	1.15	1.20	1.15	1.13
98.0	2.2267	1.19	1.18	1.15	1.20	1.15	1.17
103.0	2.2828	1.20	1.18	1.25	1.19	1.19	1.20
108.5	2.3429	1.40	1.30	1.32	1.38	1.35	1.35
113.3	2.3942	1.40	1.42	1.40	1.40	1.35	1.39

2900 µm

- **500 g**

ΔP Orifice (mm H_2o)	Superficial Velocity (m/s)	Particle Velocity (m/s)					
35.5	1.3402	0.70	0.70	0.65	0.65	0.65	0.67
40.5	1.4314	0.70	0.65	0.70	0.70	0.65	0.68
45.5	1.5172	0.65	0.70	0.75	0.75	0.70	0.71
50.0	1.5905	0.80	0.85	0.85	0.80	0.82	0.82
55.5	1.6757	1.00	1.15	1.00	1.25	1.00	1.08
60.5	1.7495	1.15	1.15	1.15	1.15	1.15	1.15
65.0	1.8134	1.20	1.25	1.25	1.25	1.25	1.24
70.0	1.8819	1.30	1.30	1.25	1.25	1.30	1.28
75.0	1.9480	1.30	1.35	1.30	1.40	1.45	1.36
80.3	2.0156	1.50	1.40	1.45	1.50	1.40	1.45
85.5	2.0798	1.40	1.45	1.45	1.50	1.60	1.48
90.5	2.1398	1.55	1.50	1.50	1.50	1.50	1.51
95.3	2.1958	1.60	1.60	1.65	1.60	1.65	1.62

- **750 g**

ΔP Orifice (mm H_2o)	Superficial Velocity (m/s)	Particle Velocity (m/s)					
55.2	1.6712	0.60	0.70	0.70	0.70	0.65	0.67
60.3	1.7467	0.85	0.80	0.78	0.75	0.80	0.80
65.5	1.8204	0.75	0.75	0.78	0.75	0.70	0.75
70.5	1.8886	0.78	0.75	0.70	0.75	0.80	0.76
75.0	1.9480	0.75	0.80	0.80	0.75	0.80	0.78
80.5	2.0181	0.75	0.80	0.85	0.80	0.85	0.81
85.5	2.0798	0.85	0.80	0.85	0.85	0.80	0.83
90.5	2.1398	0.90	0.90	0.90	0.90	1.00	0.92

Particle Shape

Spherical (3900 μm)

- **1000 g**

ΔP Orifice (mm H_2o)	Superficial Velocity (m/s)	Particle Velocity (m/s)					
66.0	1.8273	0.50	0.53	0.50	0.55	0.50	0.52
70.0	1.8819	0.60	0.55	0.50	0.50	0.53	0.54
75.0	1.9480	0.55	0.60	0.65	0.60	0.60	0.60
80.0	2.0118	0.60	0.65	0.65	0.60	0.68	0.64
85.0	2.0738	0.60	0.65	0.63	0.70	0.70	0.66
90.0	2.1339	0.70	0.65	0.70	0.70	0.65	0.68
95.2	2.1947	0.72	0.70	0.65	0.72	0.70	0.70
100.0	2.2493	0.70	0.70	0.70	0.70	0.72	0.70
106.0	2.3158	0.72	0.78	0.70	0.75	0.70	0.73

Spheroidal

- **500 g**

ΔP Orifice (mm H_2o)	Superficial Velocity (m/s)	Particle Velocity (m/s)					
53.0	1.6375	0.75	0.80	0.90	0.85	0.90	0.84
58.0	1.7130	0.70	0.75	0.70	0.75	0.75	0.73
63.1	1.7867	0.75	0.80	0.70	0.75	0.70	0.74
68.2	1.8575	0.80	0.82	0.85	0.80	0.83	0.82
73.0	1.9218	0.88	0.85	0.95	0.85	0.80	0.87
78.0	1.9865	1.00	1.05	1.05	1.05	1.05	1.04
83.0	2.0492	1.10	1.20	1.20	1.10	1.20	1.16
88.0	2.1100	1.25	1.35	1.30	1.25	1.30	1.29
93.0	2.1691	1.30	1.25	1.40	1.40	1.30	1.33
98.0	2.2267	1.40	1.35	1.35	1.30	1.30	1.34
103.0	2.2828	1.50	1.50	1.50	1.45	1.50	1.49
108.0	2.3375	1.45	1.50	1.50	1.60	1.60	1.53

- **750 g**

ΔP Orifice (mm H_2o)	Superficial Velocity (m/s)	Particle Velocity (m/s)					
65.3	1.8176	0.70	0.70	0.70	0.70	0.70	0.70
70.1	1.8832	0.90	0.75	0.70	0.80	0.78	0.79
75.5	1.9544	0.78	0.75	0.78	0.80	0.78	0.78
80.0	2.0118	0.75	0.80	0.80	0.75	0.80	0.78
85.0	2.0738	0.85	0.70	0.85	0.80	0.85	0.81
90.0	2.1339	0.70	0.70	0.70	0.75	0.65	0.70

- **1000 g**

ΔP Orifice (mm H_2o)	Superficial Velocity (m/s)	Particle Velocity (m/s)					
70.0	1.8819	0.60	0.60	0.62	0.65	0.62	0.62
75.0	1.9480	0.65	0.60	0.62	0.63	0.63	0.63
80.0	2.0118	0.65	0.65	0.70	0.60	0.55	0.63

Cylindrical

- **500 g**

ΔP Orifice (mm H_2o)	Superficial Velocity (m/s)	Particle Velocity (m/s)					
75.0	1.9480	1.25	1.30	1.18	1.20	1.15	1.22
80.0	2.0118	1.18	1.30	1.40	1.20	1.30	1.28
85.0	2.0738	1.30	1.20	1.40	1.25	1.30	1.29
90.3	2.1374	1.30	1.40	1.45	1.45	1.50	1.42
95.0	2.1923	1.45	1.50	1.70	1.50	1.60	1.55
100.0	2.2493	1.55	1.55	1.60	1.55	1.60	1.57
105.0	2.3048	1.58	1.60	1.60	1.60	1.60	1.60
110.3	2.3623	1.65	1.65	1.65	1.65	1.65	1.65
115.3	2.4152	1.65	1.60	1.75	1.60	1.60	1.64
120.0	2.4640	1.70	1.65	1.70	1.70	1.65	1.68
125.2	2.5168	1.80	1.75	1.75	1.85	1.80	1.79
131.3	2.5774	1.80	1.85	1.85	1.85	1.80	1.83

- **750 g**

ΔP Orifice (mm H_2o)	Superficial Velocity (m/s)	Particle Velocity (m/s)					
95.0	2.1923	1.18	1.20	1.20	1.18	1.23	1.20
100.0	2.2493	1.20	1.25	1.20	1.25	1.25	1.23
105.0	2.3048	1.23	1.30	1.30	1.30	1.25	1.28
110.2	2.3612	1.35	1.30	1.35	1.30	1.35	1.33
115.0	2.4121	1.40	1.38	1.40	1.45	1.50	1.43
120.3	2.4671	1.48	1.40	1.40	1.45	1.45	1.44
126.0	2.5248	1.50	1.50	1.50	1.50	1.50	1.50
130.8	2.5725	1.50	1.55	1.52	1.50	1.52	1.52

- **1000 g**

ΔP Orifice (mm H_2o)	Superficial Velocity (m/s)	Particle Velocity (m/s)					
110.0	2.3591	1.35	1.25	1.30	1.25	1.30	1.29
115.0	2.4121	1.30	1.35	1.38	1.40	1.45	1.38
120.0	2.4640	1.45	1.40	1.40	1.30	1.30	1.37
131.7	2.5813	1.45	1.30	1.40	1.38	1.35	1.38
137.0	2.6327	1.30	1.30	1.50	1.40	1.40	1.38